Mon. Not. R. Astron. Soc. **000**, 000–000 (0000) Printed 3 September 2009 (MN LATEX style file v2.2)

Discovery of a new Wolf-Rayet star and its ring nebula in Cygnus

V. V. Gvaramadze,[1⋆] S. Fabrika,[2] W.-R. Hamann,[3] O. Sholukhova,[2] A. F. Valeev,[2] V. P. Goranskij,[1] A. M. Cherepashchuk,[1], D. J. Bomans[4] and L. M. Oskinova[3]

[1] *Sternberg Astronomical Institute, Moscow State University, Universitetskij Pr. 13, Moscow 119992, Russia*
[2] *Special Astrophysical Observatory, Nizhnij Arkhyz, 369167, Russia*
[3] *Institute for Physics and Astronomy, University Potsdam, 14476 Potsdam, Germany*
[4] *Astronomical Institute, Ruhr-University Bochum, Universitätstr. 150, 44780 Bochum, Germany*

Accepted 2009 August 3, Received 2009 July 20; in original form 2009 June 3

ABSTRACT

We report the serendipitous discovery of a ring nebula around a candidate Wolf-Rayet (WR) star, HBHA 4202-22, in Cygnus using the *Spitzer Space Telescope* archival data. Our spectroscopic follow-up observations confirmed the WR nature of this star (we named it WR 138a) and showed that it belongs to the WN8-9h subtype. We thereby add a new example to the known sample of late WN stars with circumstellar nebulae. We analyzed the spectrum of WR 138a by using the Potsdam Wolf-Rayet (PoWR) model atmospheres, obtaining a stellar temperature of 40 kK. The stellar wind composition is dominated by helium with 20 per cent of hydrogen. The stellar spectrum is highly reddened and absorbed ($E_{B-V} = 2.4$ mag, $A_V = 7.4$ mag). Adopting a stellar luminosity of $\log L/L_\odot = 5.3$, the star has a mass-loss rate of $10^{-4.7}$ $M_\odot\,yr^{-1}$, and resides in a distance of 4.2 kpc. We measured the proper motion for WR 138a and found that it is a runaway star with a peculiar velocity of $\simeq 50$ km s^{-1}. Implications of the runaway nature of WR 138a for constraining the mass of its progenitor star and understanding the origin of its ring nebula are discussed.

Key words: line: identification – circumstellar matter – stars: individual: HBHA 4202-22 – stars: Wolf-Rayet

1 INTRODUCTION

It is believed that single stars of solar metallicity with an initial mass of $\gtrsim 20 - 25$ $M_\odot$ end their lives as Wolf-Rayet (WR) stars (Vanbeveren, De Loore & Van Rensbergen 1998; Meynet & Maeder 2003). The relatively small number of massive stars and the short duration of the WR phase ($\lesssim 0.5$ Myr) makes the WR stars rare objects. The present total number of WR stars in the Galaxy does not exceed several thousands (e.g. Shara et al. 1999; van der Hucht 2001). The known population of WR stars is, however, an order of magnitude less numerous (van der Hucht 2006). The large disparity between the expected and the observed number of WR stars is mostly caused by the huge interstellar extinction in the Galactic plane, which strongly limits the traditional method for searching for WR stars using optical surveys. In this respect, the infrared (IR) observations are of high importance since the interstellar medium (ISM) is much more transparent in the IR compared with the optical.

The effectiveness of IR observations in identifying new WR stars was demonstrated by Shara et al. (2009) who carried out a near-IR narrow-band imaging survey of the inner Galactic plane to select candidate WR stars and discovered 41 new WR stars in spectroscopic follow-ups (cf. Homeier et al. 2003; Hadfield et al. 2007; Mauerhan, Van Dyk & Morris 2009). Another possible way to search for new WR (and other evolved massive) stars is through detection of their (IR) circumstellar nebulae, created after a massive star leaves the main sequence (e.g. Marston et al. 1999; Egan et al. 2002; Clark et al. 2003).

In this paper, we report the discovery of a new WN8-9h star in Cygnus via the detection of its IR nebula. We thereby add a new example to the known sample of late WN (WNL) stars with circumstellar nebulae (e.g. Esteban et al. 1993). Inspired by this discovery, we undertook an ex-

⋆ E-mail: vgvaram@mx.iki.rssi.ru (VVG); fabrika, olga, azamat@sao.ru (SF, OS, AFV); wrh, lida@astro.physik.uni-potsdam.de (WRH, LMO); goray, cher@sai.msu.ru (VPG, AMC); bomans@astro.ruhr-uni-bochum.de (DJB)

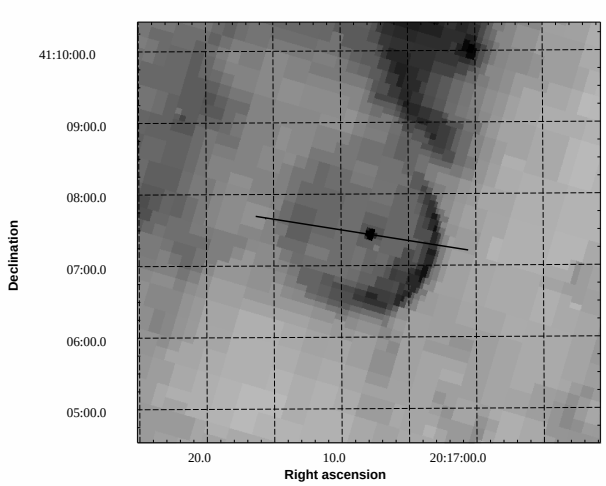

Figure 1. *Spitzer* MIPS 24 μm image of a new ring nebula in Cygnus and its central star HBHA 4202-22 (WR 138a). The orientation of the spectrograph slit in our optical observation is indicated by a line.

tensive search for similar objects using the archival data of the Spitzer Legacy Programs[1] and discovered many dozens of ring-like and bipolar IR shells (Gvaramadze, Kniazev & Fabrika 2009; cf. Carey et al. 2009). Spectroscopic follow-ups of central stars associated with two dozens of the shells showed that they are either candidate Luminous Blue Variables or related (WNL, blue supergiant) stars (Gvaramadze et al. 2009, in preparation; Kniazev et al. 2009, in preparation), which confirmed that the IR imaging provides a powerful tool for revealing evolved massive stars via detection of their circumstellar nebulae.

2 A NEW RING NEBULA AND ITS CENTRAL STAR

The nebula, which is the subject of this paper, was discovered serendipitously during our search for bow shocks around OB stars running away from star clusters in the Cygnus X region (for motivation of this search see Gvaramadze & Bomans 2008a). The nebula was detected in the archival data of the *Spitzer Space Telescope*, obtained with the Infrared Array Camera (IRAC) and the Multiband Imaging Photometer for *Spitzer* (MIPS) (Werner et al. 2004) within the framework of the Cygnus-X Spitzer Legacy Survey[2].

Fig. 1 shows the MIPS 24 μm image of the nebula and its central star. The nebula has a clear ring-like structure with a diameter of $\simeq 2.3$ arcmin and enhanced brightness along the west rim. The central star is offset for ~ 0.2 arcmin from the geometric centre of the nebula, being closer to the brightest portion of the nebula (a possible origin of the nebula and its brightness asymmetry are discussed in Section 5.2). The Cygnus-X Spitzer Legacy Survey also provides IRAC 3.6, 5.8 μm and MIPS 70 μm images of the field containing the nebula; none of them shows its signatures.

The optical counterpart to the central star was identified by Dolidze (1971) as a possible WR star due to the presence in its spectrum of an emission band around λ6750 Å. This star was included in the Catalogue of H-alpha emission stars in the northern Milky Way (Kohoutek & Wehmeyer 1999) as a candidate WR star (named in the SIMBAD database as [KW97] 44-47 or HBHA 4202-22), but was not listed in the VIIth Catalogue of Galactic Wolf-Rayet Stars (van der Hucht 2001) nor in the annex to this catalogue (van der Hucht 2006). Recently, Corradi et al. (2008) put this star in the list of candidate symbiotic stars on the basis of its IPHAS and 2MASS colours.

3 OBSERVATIONS

3.1 Spectroscopy

To verify the nature of HBHA 4202-22, we had performed spectroscopic observations with the Russian 6-m telescope using the SCORPIO[3] focal reducer (Afanasiev & Moiseev 2005) in a long-slit mode with a slit width of 1 arcsec, providing a spectral resolution of 5 Å. The orientation of the (6 arcmin long) slit is shown in Fig. 1. The spectra were taken on two occasions: 2008 October 10 (spectral range $\lambda\lambda 4000 - 5700$ Å) and 2008 November 11 (spectral ranges $\lambda\lambda 4000 - 5700$ Å and $\lambda\lambda 5700 - 7500$ Å), and reduced using standard procedures.

3.2 Photometry

Using secondary photometric standards in the regions of symbiotic variable stars V407 Cyg and AS 323 published by Henden & Honeycutt (1997), we determined accurate magnitudes of four comparison stars near HBHA 4202-22. The observations were carried out with the Special Astrophysical Observatory (SAO) 1-m Zeiss reflector and $UBVR_{\rm C}I_{\rm C}$ photometer in the good photometric night on 2009 May 29. The photometry accuracy is better than 0.02 mag. We have made expanded CCD standard star set of 18 stars to measure a DSS POSS-1 blue image. HBHA 4202-22 was measured using POSS-O plate taken in the epoch of 1954.57, CCD frames taken with the Russian 6-m telescope in 2008.90 and CCD frames taken with SAO 1-m Zeiss telescope in 2009. The results are given in Table 1.

The uniform 1-m Zeiss photometry shows that the object is variable with amplitudes between 0.04 and 0.07 in different filters in the time scale of a month. A total variability range in B filter between 1955 and 2009 is 0.19 mag. This level of variability is typical of WNL stars (e.g. Marchenko et al. 1998).

To measure the *Spizer*'s IRAC and MIPS fluxes from HBHA 4202-22, we performed aperture photometry of the star using the `MOPEX/APEX` source extraction package and applied aperture correction, obtained from the nearby bright point sources. The fluxes are listed in Table 2; the estimated

[1] http://irsa.ipac.caltech.edu/Missions/spitzer.html
[2] http://www.cfa.harvard.edu/cygnusX/index.html

[3] Spectral Camera with Optical Reducer for Photometrical and Interferometrical Observations; http://www.sao.ru/hq/lsfvo/devices/scorpio/scorpio.html

Table 1. Photometry of HBHA 4202-22 (WR 138a)

JD	B	V	$R_{\rm C}$	Source
2434951	17.15 ± 0.06	–	–	POSS-1
2454796	17.25 ± 0.01	15.44 ± 0.01	–	6-m/SCORPIO
2454981	17.34 ± 0.02	15.57 ± 0.02	13.90 ± 0.02	1-m Zeiss
2455008	17.27 ± 0.02	15.53 ± 0.02	13.85 ± 0.02	1-m Zeiss

Table 2. Details of HBHA 4202-22 (WR 138a)

RA(J2000)	$20^{\rm h}17^{\rm m}08\overset{\rm s}{.}12$
Dec.(J2000)	$41^\circ07'27\overset{''}{.}0$
l, b	78.3203, 3.1536
B (mag)	17.25 ± 0.01
V (mag)	15.44 ± 0.01
J (mag)	10.15 ± 0.02
H (mag)	9.27 ± 0.02
K_s (mag)	8.65 ± 0.02
[3.6] (mJy)	168.0 ± 5.0
[5.8] (mJy)	154.0 ± 4.6
[24] (mJy)	45.7 ± 1.4
[70] (mJy)	< 28.1

errors are $\sim 2-3$ per cent. For the flux at 70 μm, we give a 3σ upper limit since HBHA 4202-22 was not detected at this wavelength.

The details of HBHA 4202-22 are summarized in Table 2. The coordinates and the J, H, K_s magnitudes are taken from the 2MASS All-Sky Catalog of Point Sources (Skrutskie et al. 2006).

3.3 Proper motion

We measured the proper motion for HBHA 4202-22 using four epochs in the POSS-1 and POSS-2 Digitized Sky Surveys and the epoch of our 6-m/SCORPIO frames. The full epoch range is 54.3 years. 21 reference stars located within an angular radius of 2.5 arcmin from the object position were used. Typical rms deviations of reference stars in these frames are between 0.21 and 0.56 arcsec. Linear trends are well seen in both coordinates. To evaluate the stellar proper motion and its errors, we got a linear approximation of these trends using the method of least squires and derived mean rms deviations of stellar coordinates from these linear approximations. The proper motion errors were estimated by dividing these mean deviations by the epoch difference. The result is $\mu_\alpha = -4.9 \pm 1.2\,{\rm mas\,yr^{-1}}$, $\mu_\delta = -4.7 \pm 1.2\,{\rm mas\,yr^{-1}}$.

To convert the observed proper motion into the true tangential velocity of the star, we use the Galactic constants $R_0 = 8$ kpc and $\Theta = 200\ {\rm km\,s^{-1}}$ (e.g. Reid 1993; Avedisova 2005) and the solar peculiar motion $(U_\odot, V_\odot, W_\odot) = (10.00, 5.25, 7.17)\ {\rm km\,s^{-1}}$ (Dehnen & Binney 1998), and adopt a distance $d = 4.2$ kpc (see Section 4.4). We found that the star is moving in the west-southwest direction with a peculiar (transverse) velocity of $\simeq 50 \pm 24\,{\rm km\,s^{-1}}$ (here we assume that the errors are mainly due to the errors in our proper motion measurements). Note that the vector of stellar peculiar velocity is oriented by chance almost exactly along the spectrograph slit (see Fig. 1).

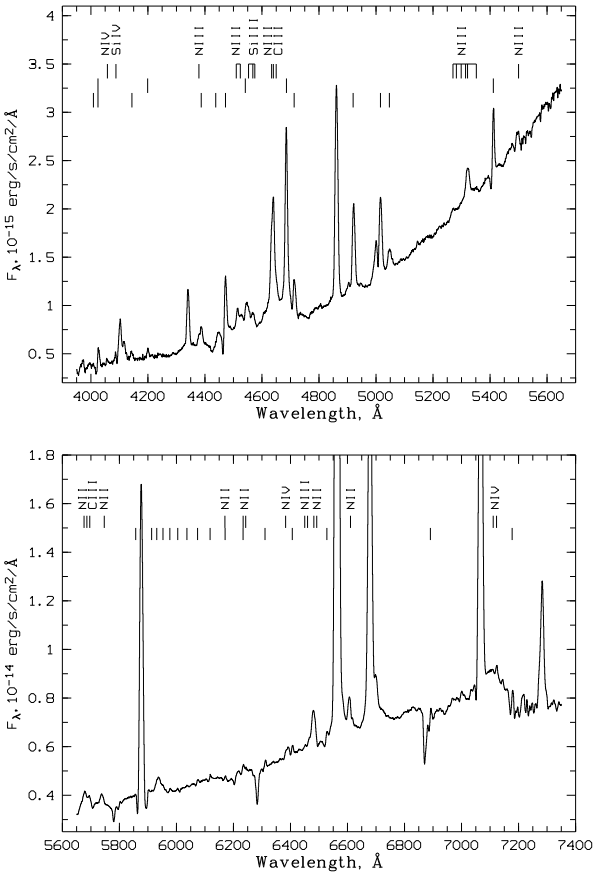

Figure 2. Blue (top) and red (bottom) spectra of HBHA 4202-22 (WR 138a) with some lines indicated (upper row). In the blue spectrum, the bottom row of vertical bars marks numerous He II lines while the middle one marks He I lines. In the red spectrum, the vertical bars mark He II lines, whereas very strong He I lines are not marked. H I emissions are not marked on both spectra as well. CCD fringes are notable at wavelengths longer than $\sim$ 6900 Å.

4 A NEW WOLF-RAYET STAR – WR 138A

4.1 Spectral type

In Fig. 2 we present the spectrum of HBHA 4202-22 in the blue and red regions. The spectrum shows strong emission lines of hydrogen, He I and He II. We detect emissions of N II, N III, C III, N IV, Si IV. No forbidden lines can be seen

in the spectrum. Many of the weaker lines in the spectrum show P Cygni profiles, while the strongest lines are entirely in emission. The strong absorptions visible in the red spectrum are telluric. Numerous diffuse interstellar bands (DIBs) are observed, in the blue region they are $\lambda\lambda 4428, 4726, 4762$, in the red the strongest one is at 6280 Å.

Our spectra also show nebular emission lines along the whole length of the slit. Radial velocity in Hα line is constant along the slit and equal to -21 ± 5 km s^{-1}. From the Balmer decrement, we estimated the interstellar extinction and obtained $A_V = 1.9 \pm 0.1$ mag (also constant along the slit), which is much less than $A_V = 7.4$ mag derived from the stellar spectrum (see Section 4.4). Hence, we conclude that the nebular line emission originates from the foreground and is not related to HBHA 4202-22 and its ring nebula.

The dominance of helium and nitrogen emission lines indicates that HBHA 4202-22 belongs to the nitrogen (WN) sequence of WR stars. The presence of hydrogen emission lines is typical for WNL subtypes (Hamann et al. 1991). We named this star WR 138a, in accordance with the numbering system of the VIIth Catalogue of Galactic Wolf-Rayet Stars by van der Hucht (2001). To determine the subtype of WR 138a more precisely, we use the classification scheme proposed by Smith (1968) and updated for WNL stars by Crowther, Hillier & Smith (1995) and Smith, Shara & Moffat (1996). The relative strengths of N III λ 4640, N IV λ 4058 and He II λ 4686 lines and the P Cygni profiles of He I lines suggest that the star belongs to the WN8-9 subtype. The WN8-9 classification for WR 138a also follows from the position of this star on the diagrams showing a comparison of the emission equivalent widths (EW) of He I λ5876 versus He II λ4686 lines and He II λ4686 EW versus FWHM for WNL stars in the Milky Way and the Large Magellanic Cloud (LMC) (see Fig. 1 of Crowther & Smith 1997). With EW(5876)=40.0 Å, EW(4686)=19.5 Å and FWHM(4686)=7.7 Å, WR 138a lies almost exactly on the line separating the WN8 and WN9 stars. The further evidence for this classification is given in Section 4.3. Following the three-dimensional classification for WN stars by Smith et al. (1996), we add a 'h' suffix to WN8-9 to indicate the presence of hydrogen emission lines, so that WR 138a is a WN8-9h star.

4.2 Radial velocity

We have measured the radial velocities of the main emission lines in the spectrum and the line widths corrected for the spectral resolution. We used the Gaussian analysis for the measurements. The accuracy of radial velocity measurements is $\lesssim 10$ km s^{-1}, while the relative velocities are measured with a notably better precision.

For hydrogen lines Hγ, Hβ and Hα, we measured heliocentric radial velocities $v_{\rm r} \simeq -10$ km s^{-1} (FWHM $\simeq 610 \pm 30$ km s^{-1}). The strongest He II λ4686 line shows $v_{\rm r} \simeq -37$ km s^{-1} (FWHM $\simeq 490$ km s^{-1}) and it does not have the P Cyg profile. All He II lines with the P Cyg profile have $v_{\rm r} \simeq 49$ km s^{-1} (FWHM $\simeq 170$ km s^{-1}) and the radial velocity measured for the absorption peak $v_{\rm a} \simeq -380$ km s^{-1}. Blue shifted absorption obviously shifts emission to the red side and makes it narrower. He I lines show the same behaviour as He II lines. The mean radial velocity for all 'non-P Cyg' He I lines is $\simeq -11$ km s^{-1} (FWHM $\simeq 590$ km s^{-1}).

We may adopt for the star's radial velocity $v_{\rm r} \sim -20$ km s^{-1}, which is an average over the hydrogen lines, He II λ4686 and the 'non-P Cyg' He I lines. It is necessary to note, however, that the radial velocity of the star cannot be determined with good accuracy, because all the spectral lines are formed in the wind. Resulting from a complicate formation process in the expanding atmosphere, the emergent line profiles are not exactly symmetric. Due to the high wind speed (700 km s^{-1}, as found in our spectral analysis, see below), these effects are large compared to possible radial velocity uncertainties.

4.3 Spectral analysis and stellar parameters

To analyze the stellar spectrum and to derive the fundamental parameters of WR 138a, we use the Potsdam Wolf-Rayet (PoWR) models for expanding stellar atmospheres. These models account for complex model atoms including iron-line blanketing in non-LTE (for a detailed description see Hamann & Gräfener 2004). For abundances of trace elements, we adopt values which are typical for Galactic WN stars – N: 0.015, C: 0.0001, Fe: 0.0014 (Hamann & Gräfener 2004).

The main parameters of a WR-type atmospheres are the stellar temperature, T_*, and the so-called transformed radius, $R_{\rm t}$. The stellar temperature T_* denotes the effective temperature related to the radius R_*, i.e. $L = \sigma T_*^4 4\pi R_*^2$, where σ is the Stefan-Boltzmann constant and R_* is by definition at a Rosseland optical depth of 20. $R_{\rm t}$ is related to the mass-loss rate $\dot{M}$ and defined by

$$R_{\rm t} = R_* \left[\frac{v_\infty}{2500 \text{ km s}^{-1}} \Big/ \frac{\sqrt{D}\dot{M}}{10^{-4} \text{ M}_\odot \text{ yr}^{-1}} \right]^{2/3} ,$$

where D is the clumping contrast (adopted here to be 4 throughout the wind as a typical value for WN stars; see Hamann & Koesterke 1998), and v_∞ is the terminal velocity of the wind.

These basic stellar parameters T_* and $R_{\rm t}$ are determined from fitting the lines in the normalized spectrum (see Fig. 3). The normalization is in fact achieved by dividing the absolutely calibrated observed spectrum by the theoretical continuum, which makes the total procedure described in the following an iterative process.

A first orientation about the proper choice of these parameters can be obtained by comparing the observed spectrum to the published grids of WN models (Hamann & Gräfener 2004). For a detailed fit, we calculate individual models for this star with the adequate terminal wind velocity, which is $v_\infty = 700$ km s^{-1} as inferred from fitting the width of the emission line profiles.

The stellar temperature is adjusted such that the balance between the lines from He I versus He II is reproduced. At the same time, R_t is adjusted, which influences the strength of the emission lines in general. The parameters of the best-fitting model are compiled in Table 3 (where for the completeness we also give the hydrogen ionising luminosity, $\Phi_{\rm i}$). Note that according to its location in the $T_* - R_{\rm t}$ plane (Hamann & Gräfener 2004), WR 138a belongs to a spectral subtype later than WN8 (cf. Section 4.1).

Fig. 3 shows that the Balmer lines of hydrogen dominate their blend with lines of the He II Pickering series. Radial velocities of the Balmer lines confirm this. These blends are

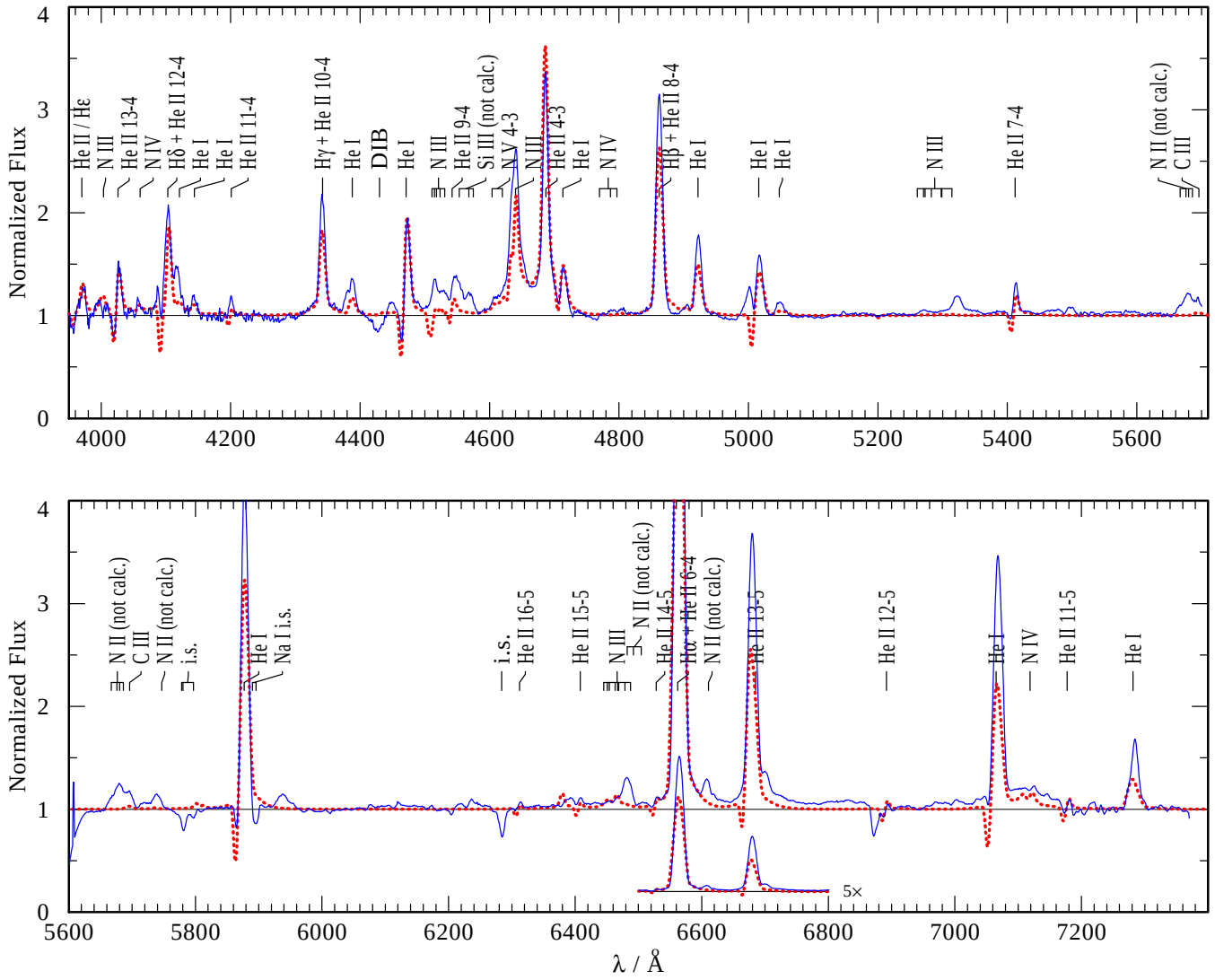

Figure 3. Observed optical spectrum (blue/solid line) of WR 138a, compared with the best fitting model (red/dotted line) with the parameters as given in Table 3. The absolutely calibrated observation had been divided by the reddened model continuum for normalization.

nicely matched by models with a hydrogen mass fraction of 20 per cent, leaving about 80 per cent of the mass for helium which is a typical composition for WNL stars.

The spectral analysis alone cannot tell the absolute dimensions of the star. These are related to the distance of the object, and will be discussed in the following subsection.

4.4 Luminosity and distance of WR 138a

The lowest plausible luminosity for a massive WNL star is about $\log L/L_\odot = 5.3$ (Hamann, Gräfener & Liermann 2006). Let us adopt this value for a moment. This choice implies the values for the stellar radius and mass-loss rate as given in Table 3. Note that, in fair approximation, WR models can be scaled to different luminosities, with $R_* \propto L^{1/2}$, $\dot{M} \propto L^{3/4}$, and $d \propto L^{1/2}$ (Schmutz, Hamann & Wessolowski 1989; Hamann & Koesterke 1998).

To estimate the corresponding distance to WR 138a, we now fit its observed spectral energy distribution (SED) with the model SED (Fig. 4). Two parameters can be adjusted for the fit, the distance d and the reddening E_{B-V}. The reddening law we adopt from Seaton (1979) in the optical and from Moneti et al. (2001) in the IR. A perfect fit to the whole SED is achieved with $E_{B-V} = 2.4$ mag, implying an extinction in the visual of $A_V = 7.4$ mag and $d = 4.2$ kpc. The strong interstellar absorption also shows up in the observed spectrum by pronounced DIBs (see Fig. 2).

The line-of-sight towards WR 138a is nearly tangential to the local (Orion) spiral arm, whose extent in this direction is $\simeq 4-6$ kpc (McCutcheon & Shuter 1970; Russeil 2003). A distance of about 4 kpc would imply that this star is located at the far end of the Orion arm, which is compatible with the high reddening.

Alternatively, one might consider if our object is in fact not a massive star with ring nebula, but a planetary nebula (PN). PN central stars with WN-type spectra are very rare; only two of them are known in our Galaxy [PMR5, Morgan, Parker & Cohen (2003) and PB 8, Todt et al. (2009)] and

Table 3. Stellar parameters for WR 138a

Spectral type	WN8-9h
T_* [kK]	40
$\log R_{\rm t}\,[R_\odot]$	0.9
$v_\infty\,[{\rm km\,s^{-1}}]$	700
$\log L\,[L_\odot]$	5.3
$R_*\,[R_\odot]$	9.4
$\log \dot{M}\,[{\rm M_\odot yr^{-1}}]$	-4.7
E_{B-V} [mag]	2.4
d [kpc]	4.2
$\log \Phi_{\rm i}\,[{\rm s^{-1}}]$	48.9

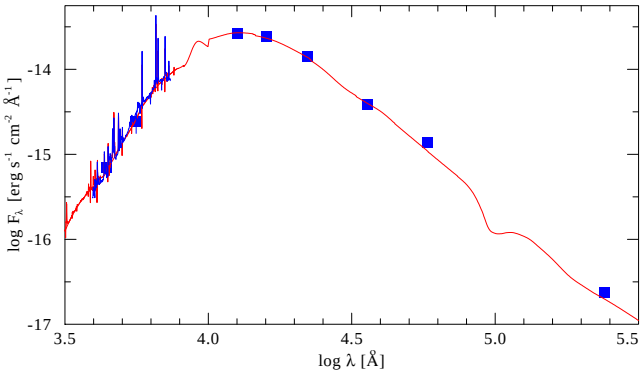

Figure 4. Observed flux distribution of WR 138a (blue/noisy) in absolute units, including the calibrated spectrum and the photometric measurements compiled in Table 2, compared to the emergent flux of the model continuum (red/smooth line), in the optical also shown with lines. The model flux has been reddened and scaled to the distance according to the parameters given in Table 3.

an eruptive one in the LMC [N 66; Hamann et al. (2003)]. With a typical luminosity of a PN central star, 6000 $L_\odot$, the photometric distance would become only 0.5 kpc, placing the object into the foreground of the Orion arm. In this case, the strong reddening would have to be of circumstellar origin. Although we cannot strictly rule out this scenario, it appears very artificial and unlikely.

The distance of $d = 4.2$ kpc, which relies on the adopted stellar luminosity of $\log L/L_\odot = 5.3$, places WR 138a at a height of 230 pc above the Galactic plane. As we will discuss in the next section, this is just compatible with the inference that WR 138a is a runaway star that has been ejected from the Galactic plane. Many WNL stars have a much larger luminosity than $\log L/L_\odot = 5.3$ (Hamann et al. 2006). A higher luminosity, however, would increase the implied distance ($d \propto L^{1/2}$) and hence lead to an even larger height above the Galactic plane, while on the other hand the evolutionary lifetime decreases with higher luminosity. Both effects together tend to make the runaway scenario impossible for much larger d and L (see Sect. 5.1). Hence, we think that our choice of $\log L/L_\odot = 5.3$ is the most plausible one.

5 DISCUSSION

5.1 WR 138a as a runaway star

Our proper motion measurements for WR 138a (Section 3.3) showed that the star is moving in the west-southwest direction (i.e. away from the Galactic plane) with a peculiar (transverse) velocity of $\simeq 50\ {\rm km\,s^{-1}}$ (for $d = 4.2$ kpc), which is typical of runaway stars. In the Galactic coordinates, the components of the peculiar velocity are almost equal to each other: $v_l \simeq -36\ {\rm km\,s^{-1}}$, $v_b \simeq 34\ {\rm km\,s^{-1}}$.

Assuming that the progenitor star of WR 138a was born near the Galactic plane and ejected from the parent star cluster soon after the birth, one has that the time it needs to reach the present height above the Galactic plane, $t_* \simeq d \sin b/v_b$, should be $\leqslant t_{\rm H}$, where $t_{\rm H}$ is the H-burning lifetime of the star. Adopting the minimum plausible luminosity for WNL stars of $\log(L/L_\odot) = 5.3$, one finds the current mass of WR 138a of $\simeq 13\ {\rm M_\odot}$, which in turn implies the initial mass of the star of $\simeq 30\ {\rm M_\odot}$ and $t_{\rm H} \simeq 6.0 - 7.0$ Myr (e.g. Meynet & Maeder 2003). Thus, one has that $t_*(\simeq 6.7\ {\rm Myr}) \lesssim t_{\rm H}$, so that the star had enough time to reach its present location.

Placing WR 138a at, for example, $d = 6$ kpc would result in a twofold increase of the stellar luminosity and in a increase of the present and initial mass of the star to, respectively, $\simeq 17\ {\rm M_\odot}$ and $\simeq 40\ {\rm M_\odot}$. In this case, $t_* \simeq 7.0\ {\rm Myr} > t_{\rm H} \simeq 4.5 - 5.5$ Myr. Further increase of d makes the discrepancy between t_* and $t_{\rm H}$ more severe. The discrepancy would be even more sever if the star spent several Myr in the parent cluster before it was ejected (Gvaramadze & Bomans 2008b; Gvaramadze, Gualandris & Portegies Zwart 2009). From this follows that the most likely initial mass of the progenitor star of WR 138a was $\simeq 25 - 30\ {\rm M_\odot}$. One cannot, however, exclude a possibility that the progenitor star was a blue straggler formed via merging of two less massive stars in the course of close binary-binary encounter, resulting in ejection of the merger product from the parent cluster (e.g. Gvaramadze & Bomans 2008b). In this case, the distance to and the mass of WR 138a could be larger.

The inference that WR 138a is a runaway star could also be used to understand the origin of its ring nebula.

5.2 Origin of the nebula around WR 138a

A runaway wind-blowing (e.g. WR) star moving through the ISM creates a highly elongated bubble (Weaver et al. 1977; Brighenti & D'Ercole 1994), whose shape in the upstream direction is determined by a ram pressure balance between the stellar wind and the ISM (Baranov, Krasnobaev & Kulikovskii 1971). The characteristic scale of the leading edge of the bubble is $R_{\rm WR} \simeq (\dot{M}_{\rm WR} v_{\rm WR}/5.6\pi m_{\rm H} n_0 v_*^2)^{1/2}$, where $\dot{M}_{\rm WR}$ and $v_{\rm WR}$ are the stellar mass-loss rate and the wind velocity, n_0 is the number density of the ambient medium, v_* is the stellar peculiar velocity and $m_{\rm H}$ is the mass of a hydrogen atom. For $\dot{M}_{\rm WR} = 10^{-4.7}\ {\rm M_\odot yr^{-1}}$ and $v_{\rm WR} = 700\ {\rm km\,s^{-1}}$ (see Table 3), $v_* = 50\ {\rm km\,s^{-1}}$ and $n_0 \simeq 0.1\ {\rm cm^{-3}}$ (typical of the ISM at $z = 230$ pc; Dickey & Lockman 1990), one finds $R_{\rm WR} \simeq 20$ pc. The small size and the nearly circular shape of the nebula around WR 138a (at $d = 4.2$ kpc, the linear radius of the nebula $r_{\rm neb} \simeq 1.4$ pc) imply that the stellar wind interacts with the dense ambient medium comoving with the star (cf. Lozinskaya 1992).

This consideration suggests that the immediate precursor of WR 138a was a red supergiant (RSG) star (i.e. the initial mass of the progenitor star was $\leqslant$ 40 $M_\odot$; cf. Section 5.1) and that the WR wind still propagates through the region occupied by the dense material shed during the RSG phase.

According to stellar evolutionary models, a massive star with the initial mass in the range from 25 to 40 $M_\odot$ evolves through the sequence O $\rightarrow$ RSG $\rightarrow$ WN (e.g. Meynet & Maeder 2003). During the RSG phase, the star loses a considerable fraction of its initial mass in the form of slow, dense wind. The subsequent fast WR wind sweeps up the RSG wind and creates a circumstellar shell. For a spherically symmetric RSG wind, the shell driven by the WR wind expands with a constant velocity (e.g. Chevalier & Imamura 1983) $v_{\rm sh} \simeq (\dot{M}_{\rm WR} v_{\rm WR}^2 v_{\rm RSG}/3\dot{M}_{\rm RSG})^{1/3}$, where $\dot{M}_{\rm RSG}$ and $v_{\rm RSG}$ are, respectively, the mass-loss rate and the wind velocity during the RSG phase. Adopting $\dot{M}_{\rm RSG} = 3\times10^{-5}\,{\rm M_\odot yr^{-1}}$ and $v_{\rm RSG} = 10$ km s^{-1} (the figures typical of RSGs), one has $v_{\rm sh} \simeq 100$ km s^{-1}, which in turn gives us the dynamical age of the nebula $r_{\rm neb}/v_{\rm sh} \simeq 1.4\times10^4$ yr. The latter estimate suggests that WR 138a only recently entered the WR phase.

The runaway nature of WR 138a allows us to propose a natural explanation of the brightness asymmetry of the nebula and the offset of the star towards the brightest portion of the nebula. Namely, we suggest that both are caused by the effect of the ram pressure of the ISM, which affects the zone occupied by the RSG wind by making it denser and more compact ahead of the star. This suggestion could be supported by an estimate of the upstream (minimum) size of the zone occupied by the RSG wind, $R_{\rm RSG} \simeq (\dot{M}_{\rm RSG} v_{\rm RSG}/5.6\pi m_{\rm H} n_0 v_*^2)^{1/2}$ ($\simeq 1.6$ pc for the parameters adopted above) $\sim r_{\rm neb}$, which shows that although the WR wind still propagates through the zone occupied by the RSG wind, it is already close to the edge of this zone to fill the density enhancement caused by the stellar motion. An additional support for our suggestion comes from the proper motion measurements for WR 138a, which show that the star is moving in the direction implied by the above consideration.

Our interpretation of the nebula around WR 138a as a circumstellar one (i.e. created via the wind-wind interaction) is consistent with the observational fact that small-scale (circumstellar) nebulae are predominantly associated with WNL stars (e.g. Lozinskaya & Tutukov 1981; Esteban et al. 1993; Barniske, Oskinova & Hamann 2008), i.e. with young WR stars, whose winds interact with the material lost during the preceding evolutionary phases rather than with the ambient ISM. The scarcity of circumstellar nebulae around WR stars suggests that they are visible on a time-scale much shorter than the duration of the WR phase. It is conceivable to associate this time-scale with the crossing-time of the region occupied by the RSG wind, i.e. $\simeq r_{\rm RSG}/v_{\rm sh} \lesssim 2-5\times10^4$ yr, where $r_{\rm RSG} = v_{\rm RSG} t_{\rm RSG} \simeq 2-5$ pc and $t_{\rm RSG} \simeq 0.2-0.5$ Myr is the duration of the RSG phase.

6 SUMMARY

We have serendipitously discovered a ring nebula around a candidate WR star, HBHA 4202-22, in Cygnus using the MIPS 24 μm data from the *Spitzer Space Telescope* archive. Our spectroscopic follow-up confirmed the WR nature of this star and showed that it belongs to the WN8-9h subtype (we named the star WR 138a). We analyzed the spectrum of WR 138a by using the Potsdam Wolf-Rayet (PoWR) model atmospheres, obtaining a stellar temperature of 40 kK. The stellar wind composition is dominated by helium with 20 per cent of hydrogen. The stellar spectrum is highly reddened and absorbed ($E_{B-V} = 2.4$ mag, $A_V = 7.4$ mag). Adopting a stellar luminosity of $\log L/L_\odot = 5.3$, the star has a mass-loss rate of $10^{-4.7}$ $M_\odot$ yr^{-1}, and resides in a distance of 4.2 kpc. We measured the proper motion for WR 138a and found that it is a runaway star with a peculiar velocity of $\simeq 50$ km s^{-1}. The runaway nature of WR 138a was used to constrain the initial mass of its progenitor star and to propose an explanation of the origin of its circular nebula. We found that the most likely initial mass of the progenitor star was $25-30$ $M_\odot$ (i.e. the immediate precursor of WR 138a was a RSG star) and suggested that the nebula around WR 138a is a circumstellar one, created via the interaction between the WR wind and the dense material shed during the preceding RSG phase.

7 ACKNOWLEDGEMENTS

We are grateful to A.Y.Kniazev for critically reading the manuscript and to the anonymous referee for useful suggestions. VVG and DJB acknowledge financial support from the Deutsche Forschungsgemeinschaft (grants 436 RUS 17/104/06 and BO 1642/14-1) for research visits of VVG at the Astronomical Institute of the Ruhr-University Bochum. SF, OS and AFV acknowledge support from the RFBR grants N 07-02-00909 and 09-02-00163. AMC acknowledges support from the RFBR grant N 08-02-01220 and the State Program of Support for Leading Scientific Schools of the Russian Federation (grant NSh-1685.2008.2). This work is based in part on archival data obtained with the *Spitzer Space Telescope*, which is operated by the Jet Propulsion Laboratory, California Institute of Technology under a contract with NASA, and has made use of the NASA/IPAC Infrared Science Archive, which is operated by the Jet Propulsion Laboratory, California Institute of Technology, under contract with the National Aeronautics and Space Administration, the SIMBAD database and the VizieR catalogue access tool, both operated at CDS, Strasbourg, France.

REFERENCES

Afanasiev V.L., Moiseev A.V., 2005, AstL, 31, 194
Avedisova V.S., 2005, ARep, 49, 435
Baranov, V.B., Krasnobaev K.V., Kulikovskii A.G., 1971, SPhD, 15, 791
Barniske A., Oskinova L.M., Hamann W.-R., 2008, A&A 486, 971
Brighenti F., D'Ercole A., 1994, MNRAS, 270, 65
Carey S.J. et al., 2009, PASP, 121, 76
Chevalier R.A., Imamura J.N., 1983, ApJ, 270, 554
Clark J.S., Egan M.P., Crowther P.A., Mizuno D.R., Larionov V.M., Arkharov A., 2003, A&A, 412, 185
Corradi R.L.M. et al., 2008, A&A, 480, 409
Crowther P.A., Smith L.J., 1997, A&A, 320, 500

Crowther P.A., Hillier D.J., Smith L.J., 1995, A&A, 293, 172
Dehnen W., Binney J.J., 1998, MNRAS, 298, 387
Dickey J.M., Lockman F.J., 1990, ARA&A, 28, 215
Dolidze M.V., 1971, Astron. Tsirk., 629, 6
Egan M.P., Clark J.S., Mizuno D.R., Carey S.J., Steele I.A., Price S.D., 2002, ApJ, 572, 288
Esteban C., Smith L.J., Vilchez J.M., Clegg R.E.S., 1993, A&A, 272, 299
Gvaramadze V.V., Bomans D.J., 2008a, A&A, 485, L29
Gvaramadze V.V., Bomans D.J., 2008b, A&A, 490, 1071
Gvaramadze V.V., Gualandris A., Portegies Zwart S., 2009, MNRAS, 396, 570
Gvaramadze V.V., Kniazev A.Y., Fabrika S., 2009, preprint (astro-ph/0909.0458)
Hadfield L.J., van Dyk S.D., Morris P.W., Smith J.D., Marston A.P., Peterson D.E., 2007, MNRAS, 376, 248
Hamann W.-R., Gräfener G., 2004, A&A, 427, 697
Hamann W.-R., Koesterke, L., 1998, A&A, 335, 1003
Hamann W.-R., Gräfener G., Liermann A., 2006, A&A, 457, 1015
Hamann W.-R., Peña M., Gräfener G., Ruiz M.T., 2003, A&A, 409, 969
Hamann W.-R., Duennebeil G., Koesterke L., Wessolowski U., Schmutz W., 1991,A&A, 249, 443
Henden A.A., Honeycutt R.K., 1997, PASP, 109, 441
Homeier N.L., Blum R.D., Pasquali A., Conti P.S., Damineli A., 2003, A&A, 408, 153
Kohoutek L., Wehmeyer R., 1999, A&AS, 134, 255
Lozinskaya T.A., 1992, Supernovae and Stellar Wind in the Interstellar Medium. Am. Inst. Phys., New York
Lozinskaya T.A., Tutukov A.V., 1981, NInfo, 49, 21
Marchenko S.V., Moffat A.F.J., Eversberg T., Morel T., Hill G.M., Tovmassian G.H., Seggewiss W., 1998, MNRAS, 294, 642
Marston A.P., Welzmiller J., Bransford M.A., Black J.H., Bergman P., 1999, ApJ, 518, 769
Mauerhan J., Van Dyk S., Morris P., 2009, PASP, 121, 591
McCutcheon W.H., Shuter W.L.H., 1970, AJ, 75, 910
Meynet G., Maeder A., 2003, A&A, 404, 975
Moneti A., Stolovy S., Blommaert J.A.D.L., Figer D.F., Najarro F., 2001, A&A, 366, 106
Morgan D.H., Parker Q.A., Cohen M., 2003, MNRAS, 346, 719
Reid M.J., 1993, ARA&A, 31, 345
Russeil D., 2003, A&A, 397, 133
Schmutz W., Hamann W.-R., Wessolowski U., 1989, A&A, 210, 236
Seaton M.J., 1979, MNRAS, 187, 73
Shara M.M., Moffat A.F.J., Smith L.F., Niemela V.S., Potter M., Lamontagne R., 1999, AJ, 118, 390
Shara M.M. et al., 2009, AJ, 138, 402
Skrutskie M.F. et al., 2006, AJ, 131, 1163
Smith L.F., 1968, MNRAS, 138, 109
Smith L.F., Shara M.M., Moffat A.F.J., 1996, MNRAS, 281, 163
Todt H., Peña M., Hamann W.-R., Gräfener, 2009, A&A, submitted
van der Hucht, K.A., 2001, New Astr. Rev., 45, 135
van der Hucht, K.A., 2006, A&A, 458, 453
Vanbeveren D., De Loore C., Van Rensbergen W., 1998, A&AR, 9, 63
Weaver R., McCray R., Castor J., Shapiro P., Moore R., 1977, ApJ, 218, 377
Werner M.W. et al., 2004, ApJS, 154, 1